PRP is highly hydrophobic (Vishwanatha et al., 1986a), as the two polypeptides are dominated by hydrophobic amino acids.

The physiological role of PRP in eukaryotic cells has not been established. They help DNA primase–polymerase α in locating either RNA or RNA–DNA primers at replication forks (Pritchard et al., 1983) and may function as proteins involved in switching from transcription of initiator RNA to replication in DNA synthesis in vivo (Vishwanatha et al., 1986b). With the availability of homogeneous PRP preparations, it should be possible to define the physiological role of these proteins.

References

Alberts, B., & Herrick, G. (1971) *Methods Enzymol. 21*, 198–217.

Baril, E., Mitchener, J., Lee, L., & Baril, B. (1977) *Nucleic Acids Res. 4*, 2641–2653.

Bradford, M. M. (1976) *Anal. Biochem. 72*, 248–254.

Campbell, J. L. (1986) *Annu. Rev. Biochem. 55*, 733–771.

Fairman, M., Prelich, G., Tsurimoto, T., & Stillman, B. (1988) *Biochim. Biophys. Acta 951*, 382–387.

Hay, R. T., & DePamphilis, M. L. (1982) *Cell 28*, 767–779.

Kornberg, A. (1980) *DNA Replication*, W. H. Freeman, San Francisco.

Kornberg, A. (1988a) *J. Biol. Chem. 263*, 1–4.

Kornberg, A. (1988b) *Biochim. Biophys. Acta 951*, 235–239.

Laemmli, U. K. (1970) *Nature (London) 227*, 680–685.

Lamothe, P., Baril, B., Chi, A., Lee, L., & Baril, E. (1981) *Proc. Natl. Acad. Sci. U.S.A. 78*, 4723–4727.

McHenry, C. S. (1988) *Biochim. Biophys. Acta 951*, 240–248.

Morrissey, J. H. (1981) *Anal. Biochem. 117*, 307–310.

Novak, B., & Baril, E. (1978) *Nucleic Acids Res. 5*, 221–239.

Prelich, G., & Stillman, B. (1988) *Cell 53*, 117–126.

Pritchard, C. G., & DePamphilis, M. L. (1983) *J. Biol. Chem. 258*, 9801–9809.

Pritchard, C. G., Weaver, D. T., Baril, E. F., & DePamphilis, M. L. (1983) *J. Biol. Chem. 258*, 9810–9819.

Sambrook, J., Fritsch, E. F., & Maniatis, T. (1989) *Molecular Cloning: a laboratory manual*, 2nd ed., Cold Spring Harbor Laboratory Press, N.Y.

Siegel, L. M., & Monty, K. J. (1966) *Biochim. Biophys. Acta 112*, 346–362.

Tsurimoto, T., & Stillman, B. (1989) *Mol. Cell. Biol. 9*, 609–619.

Vishwanatha, J. K., & Baril, E. F. (1986) *Nucleic Acids Res. 14*, 8467–8487.

Vishwanatha, J. K., Coughlin, S. A., Owen, M. W., & Baril, E. F. (1986a) *J. Biol. Chem. 261*, 6619–6628.

Vishwanatha, J. K., Yamaguchi, M., DePamphilis, M. L., & Baril, E. F. (1986b) *Nucleic Acids Res. 14*, 7305–7323.

Weaver, D., & DePamphilis, M. L. (1982) *J. Biol. Chem. 257*, 2075–2086.

Wold, M. S., Weinberg, D. H., Virsheup, D. M., Li, J. J., & Kelly, T. (1989) *J. Biol. Chem. 264*, 2801–2809.

Wong, S. W., Syvaoja, J., Tan, C.-K., Downey, K. M., So, A. G., Linn, S., & Wang, T. S.-F. (1989) *J. Biol. Chem. 264*, 5924–5928.

Yuen, S. W., Chui, A. H., Wilson, K. J., & Yuan, P. M. (1989) *BioTechniques 7*, 74–83.

DNA Repair within Nucleosome Cores of UV-Irradiated Human Cells†

Karen A. Jensen and Michael J. Smerdon*

Biochemistry/Biophysics Program, Washington State University, Pullman, Washington 99164-4660

Received December 8, 1989; Revised Manuscript Received February 14, 1990

ABSTRACT: We have compared the distributions of repair synthesis and pyrimidine dimers (PD) in nucleosome core DNA during the early (fast) repair phase and the late (slow) repair phase of UV-irradiated human fibroblasts. As shown previously [Lan, S. Y., & Smerdon, M. J. (1985) *Biochemistry 24*, 7771–7783], repair synthesis is nonuniform in nucleosome core particles during the fast repair phase, and the distribution curve can be approximated by a model where repair synthesis occurs preferentially in the 5′ and 3′ end regions. In this report, we show that, during the slow repair phase, [^{3}H]dThd-labeled repair patches are much more uniformly distributed in core DNA, although they appear to be preferentially located in sequences degraded slowly by exonuclease III. This change in distribution cannot be explained by an increase in patch size during slow repair, since the size of these patches actually decreases to about half the size measured during the fast repair phase. Furthermore, PD mapping within core DNA at the single-nucleotide level demonstrated that, at least within the 30–130-base region from the 5′ end, there is little (or no) selective removal of PD during the fast repair phase. However, the nonuniform distribution of repair synthesis obtained during fast repair throughout most of the core DNA region (~40–146 bases) is accounted for by the nonuniform distribution of PD in core DNA. The near-uniform distribution of repair synthesis observed during slow repair may result from more extensive nucleosome rearrangement and/or nucleosome modification during this phase.

Excision repair of ultraviolet (UV)[1] damage to DNA of human cells is associated with at least two distinct phases [reviewed in Smerdon (1989)]. Between 50 and 75% of the pyrimidine dimers (PD) are removed rapidly from the genome, and the remaining PD are removed much more slowly. During each of these phases, the repair process is associated with nucleosome rearrangements and, following repair synthesis and ligation, newly repaired regions rapidly become associated with

† This study was supported by NIH Grant ES02614. The laser densitometer used in these studies was purchased with funds provided by NSF Grant PCM 8400841.

[1] Abbreviations: PD, cis-syn cyclobutane pyrimidine dimers; UV, ultraviolet; ESS, endonuclease-sensitive sites.

0006-2960/90/0429-4773$02.50/0

nucleosome structures (Smerdon, 1989).

We reported previously (Lan & Smerdon, 1985) that, during the fast repair phase in human fibroblasts, repair patches are nonuniformly distributed in nucleosome core DNA following their "maturation" into nucleosomes. A good approximation of this distribution is obtained by a simple model where preferential repair synthesis occurs in ~60 bases at the 5′ end and ~30 bases at the 3′ end of the core particle (Lan & Smerdon, 1985). One explanation for this correlation is that the fast phase may involve repair of the ~90 bases in these end regions (as well as nucleosome linker DNA) and the slow phase may involve repair of the ~50-base central region of nucleosomes, which is least accessible to DNase I cutting in vitro [see discussion in Lan and Smerdon (1985)]. This model for excision repair in nucleosomes makes several testable predictions. For instance, the distribution in nucleosome core DNA of repair patches inserted during the slow repair phase should differ from that observed during the fast repair phase. This difference will depend on the size of repair patches inserted during each phase. For example, if the patch size during the slow phase is the same as during the fast phase and nucleosomes re-form in the same position on repaired DNA as before repair occurred, then the distribution of repair patches in core DNA should be heavily weighted toward the central region. Another prediction of the model is that PD should be removed more rapidly from the 5′ and 3′ end regions of nucleosome cores than from the ~50-base central region.

Since selective repair at the nucleosome level could have important implications for mutagenesis and (possibly) neoplastic transformation (Bohr et al., 1987), we have extended the distribution analysis of repair synthesis in core DNA to the slow repair phase in human fibroblasts. Second, we have performed direct measurements of the repair patch size for each repair phase. Third, we have employed a sensitive mapping procedure to determine the yield of PD in nucleosome core DNA at the single nucleotide level (Gale et al., 1987; Gale & Smerdon, 1988). This procedure involves digestion of 5′-end-labeled core DNA fragments from UV-irradiated chromatin with T4 polymerase–exonuclease, which is quantitatively blocked by PD and the minor UV photoproduct (6-4) pyrimidine–pyrimidone (Doetsch et al., 1985; Chan et al., 1985). Surprisingly, the formation of PD in core particle DNA was found to be strongly modulated with an average period of 10.3 bases (Gale et al., 1987; Gale & Smerdon, 1988). This pattern is entirely due to the major class of UV photoproducts (PD), since the distribution of (6-4) photoproducts is nearly random in the nucleosome core region (Gale & Smerdon, 1990). We have used this method to directly map the PD distribution in nucleosome cores of human chromatin and follow the disappearance of PD during repair. Finally, we have tested the possibility that the nonuniform distribution of repair synthesis in core DNA observed during the fast phase reflects the nonuniform distribution of PD in this region.

Materials and Methods

Cell Culture and Prelabeling. Human diploid fibroblasts (strains AG1518 and IMR-90) were grown in Dulbecco's modified Eagle's medium supplemented with 5% fetal bovine serum and 5% newborn calf serum, as previously described (Smerdon et al., 1982). Cells were grown in 10% CO_2 and were routinely checked for mycoplasma contamination (Gene-Probe hybridization test).

The DNA was prelabeled (uniformly) by incubating cells for 1 week with 1–75 nCi/mL [^{14}C]dThd (Du Pont NEN; 40–60 mCi/mmol) or 10 nCi/mL [^{3}H]dThd (Du Pont NEN; 50–90 Ci/mmol), depending on the experiment, immediately after a 1:3 split. Following this time, the radioactive medium was replaced with complete medium, not containing label, and the cells were grown to confluence (2–3 weeks after passage).

UV Irradiation and Repair Labeling. Confluent monolayers were irradiated in Petri dishes with (predominantly) 254-nm light by using a germicidal lamp (Sylvania, Model G30T8), as previously described (Smerdon et al., 1978). Irradiations were carried out in a 37 °C room, and the total dose given was 12 J/m^2 at a flux of 2 W/m^2 (measured with an Ultraviolet Products, Inc., UV meter, Model J-225).

For total genome repair incorporation experiments, prelabeled AG1518 cells were labeled for 3 h at various times after irradiation in the presence of 20 μCi/mL [^{3}H]dThd and 50 μM BrdUrd, with or without 2 mM hydroxyurea. Cells were harvested and nuclei isolated as described previously (Smerdon et al., 1979). Nuclei were then suspended in 10 mM Tris·HCl (pH 7.4), 10 mM EDTA, 10 mM NaCl, and 0.5% SDS and digested with 100 μg/mL proteinase K (E. Merck) overnight at 37 °C. The resulting DNA was sheared by several passages through a 23-gauge needle and centrifuged to equilibrium in an alkaline CsCl gradient and the parental density DNA isolated for scintillation counting (Smerdon et al., 1979). Centrifugation was carried out at 20 °C in a Beckman 70.1 Ti rotor at 50 000 rpm for 24 h.

Assay for Endonuclease-Sensitive Sites. The general protocol for measuring UV-induced endonuclease-sensitive sites (ESS) has been described in detail by others (Ganesan et al., 1981; Paterson et al., 1981). Our experiments were performed as described in Smerdon et al. (1982), with the modification that cell pellets were incubated with (or without) the enzyme T4 endonuclease V, which has absolute specificity for PD (Friedberg, 1985). This enzyme was prepared from a clone of the *denV* gene of phage T4 obtained from Drs. K. Valerie and J. deRiel, Temple University (A. Murad and M. Smerdon, unpublished results). The alkaline sucrose density gradient profiles were analyzed as described previously (Smerdon et al., 1982) to obtain the number of ESS/10^8 daltons.

Mapping Repair Synthesis and PD in Core DNA. For determination of the distribution of repair patches in core DNA, confluent cultures were prelabeled with 75 nCi/mL [^{14}C]dThd for fast repair and 25 nCi/mL [^{14}C]dThd for slow repair to uniformly label the heterogeneous population of nucleosomes in the genome. Cells were incubated with 10 μCi/mL [^{3}H]dThd during each repair phase (repair label). Nuclei preparation, mononucleosome isolation, and preparative electrophoresis of 146 bp core DNA were performed as described in detail elsewhere (Lan & Smerdon, 1985). Core DNA samples were digested with *Escherichia coli* exonuclease III (Bethesda Research Laboratories) at a final concentration of 6–12 units/μg of DNA for 50–90 min at 37 °C to yield different extents of digestion. The resulting digestion products, containing the original 5′ end, were separated on denaturing polyacrylamide gels, and the ^{3}H and ^{14}C profiles of these products were analyzed as described (Lan & Smerdon, 1985).

PD mapping in core DNA was performed as described previously (Gale et al., 1987; Gale & Smerdon, 1988). For these experiments, 146-base core DNA was prepared on denaturing gels to eliminate the high background of nonspecific single-strand breaks which artifactually weight the 5′ end (Gale & Smerdon, 1988).

Repair Patch Size Measurements. Repair patch size was measured as described by Smith et al. (1981) with some modifications (K. Sidik and M. Smerdon, submitted for publication). Briefly, confluent cells, prelabeled with [^{14}C]-dThd, were incubated for 2 h in 50 μM BrdUrd and 45 min

in 2 mM hydroxyurea prior to irradiation. After irradiation, cells were labeled with 20 μCi/mL [^{3}H]dCyd (ICN Biomedicals; 20–30 Ci/mmol), in the presence of BrdUrd and hydroxyurea, for 2–6 h during the fast or slow repair phase. To allow ligation of all labeled repair patches, the medium was then replaced for 1 h with conditioned medium containing 50 μM (unlabeled) dCyd (i.e., chased). High molecular weight DNA was isolated and sheared, as described above for repair incorporation experiments, and centrifuged to equilibrium in an alkaline CsCl gradient (0.1 M K_2PO_4, pH 12.5; solution density of 1.7719 gm/cm^3). Centrifugation was carried out in a Beckman VTi65 rotor at 50 000 rpm for 16 h at 25 °C in a Beckman L8-70 ultracentrifuge. The parental density peak was pooled and sonicated by using 15 pulses (30 s each) with a Tekmar Sonicator and microtip using a power setting of 4. The sample density was then adjusted to 1.705 gm/cm^3 with 0.1 M K_2PO_4 (pH 12.5), and a second centrifugation was performed in a VTi65 rotor at 40 000 rpm for 40 h at 25 °C. The median size of the sonicated DNA was determined from electrophoresis on 2% agarose gels, using *Hpa*II-digested pBR322 DNA as markers, and quantitative scanning of photographic negatives (K. Sidik and M. Smerdon, submitted for publication). The separation (in fractions) of completely substituted DNA from parental density DNA was also determined for the patch size calculations.

Peak Deconvolution Analysis of PD Distributions. Autoradiograms of PD mapping gels were scanned with a laser densitometer (LKB Ultroscan XL, Model 2222) and the scans digitized with an electronic *x,y* coordinate digitizer (Alteek Data Tab, Model 8C40) and IBM PS/2 computer (Model 60) using software from Jandel Scientific (Sigma Scan). The digitized ensemble peaks were analyzed on a Nicolet 1280 computer using the NMCCAP program for curve analysis and deconvolution. The relative area for each ensemble peak was then determined (Lan & Smerdon, 1985). The best fit to the profiles (lowest rms values) were obtained with a basis spectrum line shape of 50% Gaussian and 50% Lorentzian.

Results

Time Course of Total Repair Synthesis and PD Removal. Two different human fibroblast strains (IMR-90 and AG1518) were chosen for these studies, since our previous observations indicated they may differ considerably in their overall repair kinetics (unpublished results) and, therefore, may have different combinations of fast and slow repair components. To determine the appropriate time frames in which to study fast and slow repair at the nucleosome level in each cell type, the kinetics of excision repair of the genome as a whole was examined by monitoring both repair synthesis and PD removal at different times after UV irradiation. The time course of repair synthesis for IMR-90 cells has been reported previously (Smerdon et al. 1978). As discussed in that report, the rapid phase of repair synthesis lasts only 2–3 h in these cells. By 6 h after irradiation, the rate decreases by a factor of 12 and remains constant for at least 35 h. The level of PD was measured following different repair times by using the enzyme T4 endonuclease V, which produces single-strand cuts specifically at PD, and the number of enzyme-sensitive sites (ESS) was determined on alkaline sucrose gradients (Ganesan et al., 1981; Paterson et al., 1981). As expected, the time course of PD removal reflected the time course for repair synthesis with a sharp break in the data between 2 and 3 h (data not shown). The data also indicated that ~50% of the PD are removed during the rapid phase in these cells. These results indicate that the fast repair phase is over by 6 h after UV irradiation in IMR-90 cells.

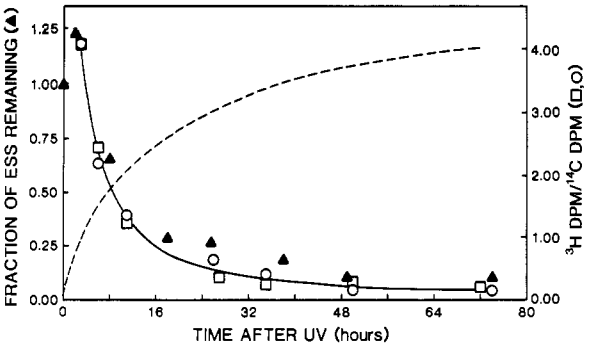

FIGURE 1: Time course of repair synthesis and PD removal for AG1518 cells. For repair synthesis measurements, confluent cells, prelabeled with [^{14}C]dThd, were pulse-labeled with [^{3}H]dThd and BrdUrd for 3 h in the presence (○) or absence (□) of 2 mM hydroxyurea at different times after UV irradiation. The DNA was centrifuged to equilibrium on alkaline CsCl gradients, and the ^{3}H and ^{14}C dpm of the parental density peak was determined. The ^{3}H/^{14}C ratio is a measure of the repair synthesis occurring during each 3-h pulse. The fit to these data (solid line) approximatly defines a derivative curve for repair accumulation. The integral curve taken from this fit (dashed line) approximately defines the time course of repair synthesis. The number of endonuclease-sensitive sites (ESS) in DNA were determined from digestion of total cellular DNA with and without T4 endonuclease V, which cuts specifically at PD, and subsequent centrifugation on alkaline sucrose gradients (Materials and Methods). The values shown (▲) represent the fraction of ESS compared to 0 time.

The time course for repair synthesis in AG1518 cells was measured by pulse labeling cells at various times after UV irradiation. For these experiments, confluent cells, labeled uniformly during growth with [^{14}C]dThd, were pulse-labeled with [^{3}H]dThd and BrdUrd during repair. The parental density DNA was isolated on alkaline CsCl gradients and the ^{3}H dpm/^{14}C dpm ratio (repair synthesis) was determined. This protocol was used to more accurately measure the repair synthesis time course in these cells, since our past experience suggested that the fast and slow phases of repair were less well-defined compared to IMR-90 cells (unpublished observations). As shown in Figure 1 (open symbols), this is indeed the case. The decrease in the data is almost monophasic with time, and the same time dependence is observed whether or not the cells are treated with 2 mM hydroxyurea. Since these data approximate a derivative curve of the repair accumulation, they indicate that there is no distinct break between the fast and slow phases, as observed for IMR-90 cells. The predicted accumulation of repair synthesis (dashed line) indicates that the fast phase lasts longer in these cells and may not be complete until 16–24 h after irradiation. The time dependence for removal of PD is also shown in Figure 1 (triangles). As in the case of IMR-90 cells, these data reflect the time course obtained for repair synthesis. A fit to these data reveals a possible break in the curve at about 17 h (fit not shown), or about 6–8-fold longer than the time where a clear break is observed for IMR-90 cells. These latter results also indicate that ~70% of the PD sites are repaired during the fast phase in these cells.

Distribution of Repair Synthesis in Core DNA. Previously, we reported a method for analyzing the distribution of repair synthesis in nucleosome core DNA (Lan & Smerdon, 1985). We have used this method to compare the distributions of repair synthesis obtained during the two repair phases. Once again, AG1518 cells were labeled with [^{14}C]dThd during growth, grown to confluence, irradiated with 12 J/m^2 UV light, and labeling during the fast or slow repair phase with [^{3}H]-dThd. Nucleosome core DNA (146 bp) was then isolated and digested to different extents with *E. coli* exonuclease III (a

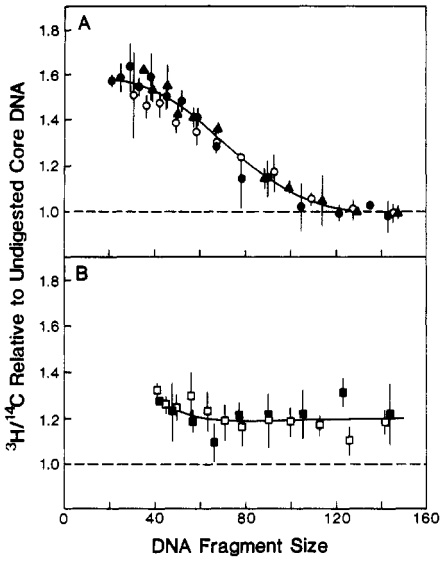

FIGURE 2: Distribution of repair synthesis in nucleosome core DNA during early (A) and late (B) times after UV irradiation. (A) Confluent cells, prelabeled with [^{14}C]dThd, were labeled with [^{3}H]dThd immediately after UV irradiation for 30 min (▲), 3 h (○), or a 30-min pulse plus a 2.5-h chase period (●). Isolated 146 bp core DNA was digested with exonuclease III, and the fragments were separated on denaturing gels (Materials and Methods). The data represent the $^3H/^{14}C$ ratio of different sized fragments divided by this ratio for undigested core DNA. (B) Same as in panel A except cells were labeled with ^{3}H during the periods of 20–24 h (□) or 48–51 h (■) after irradiation. Error bars were determined as described in Lan and Smerdon (1985).

3′ → 5′ double-strand-specific exonuclease). Following electrophoresis on denaturing polyacrylamide gels, the lanes were cut out and sliced and the slices assayed for radioactivity. Due to the long prelabeling period (1 week), either one or both of the DNA strands of most cells should be labeled with ^{14}C and the distribution of this label should be uniform between the 5′ and 3′ ends of the heterogeneous population of core DNAs. Since exonuclease III digestion creates a series of DNA fragments all containing the original 5′ end of the core DNA, the resulting $^3H/^{14}C$ ratio as a function of DNA size gives an indication of the distribution of repair synthesis within core DNA and should be constant for a uniform distribution of repair label (Lan & Smerdon, 1985).

In agreement with previous results (Lan & Smerdon, 1985; Nissen et al., 1986), cells labeled during the early, rapid phase yield a $^3H/^{14}C$ profile that is not uniform but has a sigmoidal dependence on DNA fragment size (Figure 2A). This is the case for cells labeled for 30 min (triangles), 3 h (open circles), or 30 min plus a 2.5-h chase period (closed circles). This profile indicates that repair incorporation is enhanced in the 5′ end of nucleosome core DNA, and the sigmoidal shape indicates that some enhanced repair synthesis also occurs in the 3′ end (Lan & Smerdon, 1985). This distribution is "stable" during a 3-h period, although it gradually becomes randomized during much longer times (Nissen et al., 1986). (It should be noted that this assay does not distinguish between individual strands and the profile obtained is the average distribution for both strands of core DNA.)

In order to assess the distribution of repair patches inserted during the slow repair phase, AG1518 cells were labeled for 3 or 4 h, starting at 20 or 48 h after irradiation (Figure 2B). In this case, a nearly constant $^3H/^{14}C$ ratio is observed over the DNA size range measured (40–146 bases from the 5′ end). We note that the range of sizes is reduced from that shown in Figure 2A due to the lower level of repair incorporation during the slow repair pulses (Figure 1), which does not allow accurate determination of the $^3H/^{14}C$ ratio for sizes <40 bases. These data indicate that repair patches inserted during the slow repair phase are distributed more randomly in nucleosome cores than patches inserted during the fast repair phase. Another feature of the data is that the relative $^3H/^{14}C$ ratio is >1.0 for all DNA sizes. This may reflect a sequence bias for repair occurring at late times (i.e., repair during the slow phase may occur preferentially in sequences that are most resistant to exonuclease III digestion). Thus, sequences that are rapidly degraded by exonuclease III (Linxweiler & Horz, 1982) are removed from the core DNA population after very little digestion, and these sequences may contain a much smaller fraction of [^{3}H]dThd-labeled repair patches (per unit DNA) than the remaining sequences, which are degraded more slowly.

Repair Patch Size during Early and Late Times. There are several possible explanations for the difference in repair patch distribution in nucleosome cores between early and late times after irradiation (Figure 2). One explanation is that the size of repair patches inserted during the slow repair phase is much larger than the size of patches inserted during early times (see Discussion). To examine this possibility, we measured the patch size in both AG1518 and IMR-90 cells for repair occurring during each repair phase. Patch size measurements were performed by using the BrdUrd density-shift method [reviewed in Smith et al. (1981)], which relies on the shift from parental density of short (250–350 bp) DNA fragments that are labeled only by repair synthesis. Cells were labeled with [^{14}C]dThd during growth (parental density label), grown to confluence, and repair labeled with [^{3}H]dThd in the presence of BrdUrd (repair patch density label). Initially, large DNA fragments were purified and run on alkaline CsCl gradients to separate newly replicated DNA (heavy peak) from repaired DNA (light peak). This step was especially important for AG1518 cells labeled at late times, since the majority of ^{3}H label was incorporated via replicative synthesis (data not shown).

Once purified on the initial alkaline CsCl gradient, the DNA was fragmented to average sizes of 230–300 bp by sonication, and the samples were run on a second alkaline CsCl gradient (Figure 3). As expected, the repair-labeled DNA fragments banded at heavier densities than the parental density fragments. However, for each cell strain, the shift observed for DNA from cells labeled during late times (slow repair) was less than that observed for DNA labeled at early times (Figure 3), indicating that the average patch size at late times is actually less than that at early times. The patch sizes were determined from the shift measured on these gradients compared to the shift obtained for fully substituted DNA, and from the median size of the fragments (Table I). As can be seen, the average size of repair patches inserted at early times is about twice that of patches inserted later on in repair.

Distribution of PD in Core DNA during Repair. To test for selective repair in the 5′ and 3′ end regions of core DNA (see the introduction), we examined the PD distribution within core DNA at the single nucleotide level in each cell strain (Gale et al., 1987; Gale & Smerdon, 1988). This procedure involves (1) isolating a near homogeneous sized population of single-strand (146-base) core DNA fragments from staphylococcal nuclease digested nuclei, (2) removing 3′-phosphates with calf intestinal phosphatase, (3) 5′ end labeling the fragments with ^{32}P, (4) digesting the fragments with T4 polymerase–(3′→5′)-exonuclease, which is blocked by the major UV photoproducts (Doetsch et al., 1985; Chan et al., 1985), and (5) separating the resulting fragments on gels and per-

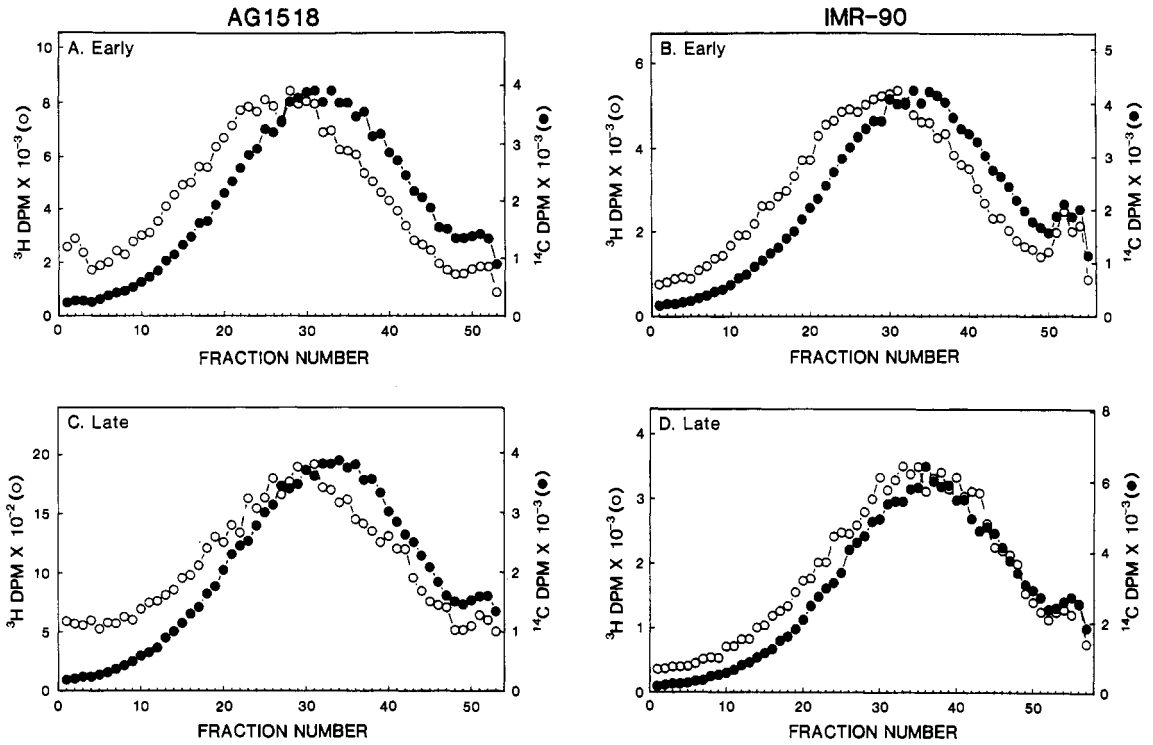

FIGURE 3: Alkaline CsCl gradient profiles of sonicated DNA. For fast repair (early), both AG1518 (A) and IMR-90 (B) cells were labeled for 2 h immediately after UV irradiation. For slow repair (late), AG1518 cells were labeled from 40 to 46 h after irradiation (C), and IMR-90 cells were labeled from 24 to 30 h after irradiation (D). Large DNA of parental density was isolated on an alkaline CsCl gradient, sonicated to an average size of 230–300 bases (AG1518 cells) or 240 bases (IMR-90 cells), and recentrifuged to equilibrium in alkaline CsCl gradients. In each panel, the ^{14}C dpm profile (●) denotes the banding of parental density (prelabeled) DNA.

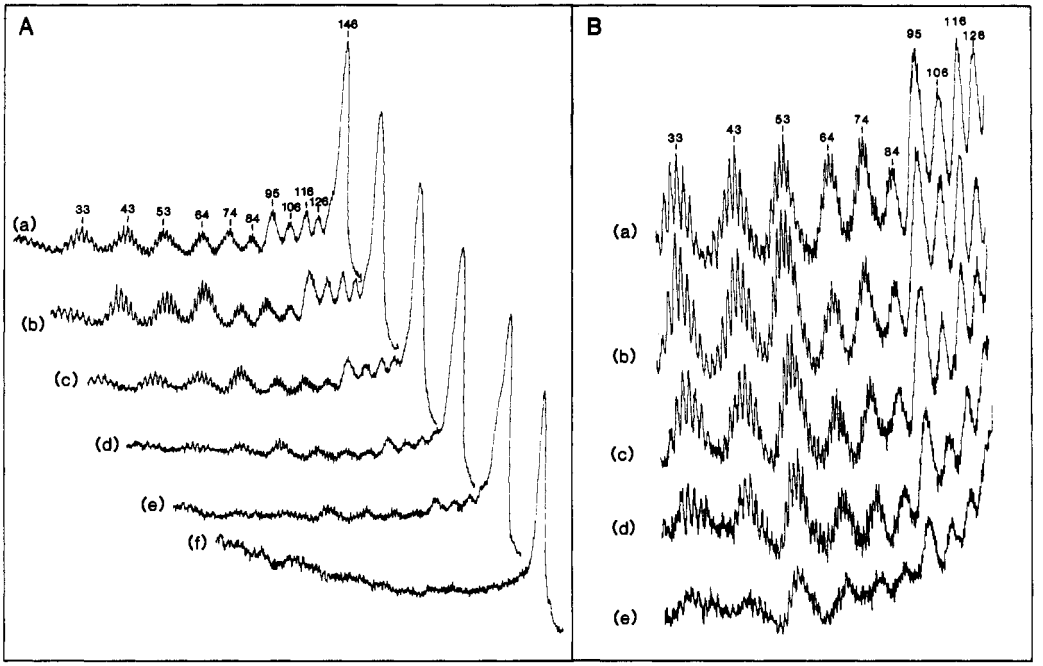

FIGURE 4: Distribution of PD in nucleosome core DNA from AG1518 cells following different repair times. (A) Densitometer scans of T4 polymerase–exonuclease digestion profiles of 146-base core DNA. Scans are for cells that were irradiated and incubated for (a) 0, (b) 7, (c) 24, (d) 48, or (e) 72 h prior to harvest. Scan f is for core DNA that was isolated from unirradiated cells and irradiated as naked DNA. Migration is from right to left. Numbers above scan a indicate peak positions (in bases) from the 5′ end of core DNA and were determined from the position of UV-irradiated, T4 polymerase–exonuclease digested marker fragments (Gale et al., 1987). (B) Magnification of the central (30–130-base) region of the scans shown in panel A where the scans are aligned for direct comparison.

forming autoradiography. This procedure is quite sensitive since fragments not containing PD are digested to small oligonucleotides, which are removed prior to running the gel (Gale & Smerdon, 1988). Therefore, these fragments do not interfere with the resulting autoradiogram. Thus, we were able to measure PD distributions at the same UV dose (12 J/m^2) used for the repair synthesis mapping experiments, where the repair response is not saturated in these cells (Smith & Okumoto, 1984; Cohn & Lieberman, 1984). At this UV dose, the photoproduct yield decreases from 1 PD every 20–30 nucleosomes, immediately after irradiation (Gale & Smerdon, 1988; Ramanathan & Smerdon, 1989), to a level of 1 PD every

Table I: Size of Repair Patches Incorporated during Early and Late Repair Times in Human Cells

cells	phase	DNA size[a] (bases)	fraction shift[b]	patch size[c] (bases)
AG1518	early	300	4.4	28
AG1518	late	230	3.0	15
IMR-90	early	240	3.7	19
IMR-90	late	240	1.7	9

[a] The median size of sonicated DNA was determined by agarose gel electrophoresis using fragments from a digest of pBR322 with *HpaII* as size standards (Sidik and Smerdon, submitted for publication). [b] Determined from the gradient profiles in Figure 5 as described in Walker and Th'ng (1982). [c] The average patch size ($\langle B \rangle$) was calculated from the expression

$$\langle B \rangle = L_{med}(\Delta\rho/\Delta\rho_0)$$

where L_{med} is the median length of sonicated DNA, $\Delta\rho$ is the separation (in fractions) of repair-labeled DNA and parental density DNA, and $\Delta\rho_0$ is the separation (in fractions) of completely substituted DNA and parental density DNA. This latter difference ($\Delta\rho_0$) was 48 fractions and 49 fractions for AG1518 cells and IMR-90 cells, respectively.

200–300 nucleosomes following 72 h of repair (Figure 1).

The results of this analysis for AG1518 cells are shown in Figure 4 following different extents of repair. Immediately after UV irradiation (Figure 4A, scan a), the pattern of PD for all but the 3′ end is similar to that reported for isolated chromatin irradiated at higher UV doses (Gale et al., 1987; Gale & Smerdon, 1988). As shown in those reports, the yield of PD in nucleosome cores is modulated, having an average periodicity of 10.3 bases, and the sites of high PD yield are located at positions where the DNA strand is farthest from the histone surface. The large peak at the 3′ end of the scans shown in Figure 4A represents core DNA fragments which were resistant to exonuclease cleavage. These fragments represent a small fraction of the total core DNA population but are more pronounced in the exonuclease-resistant fraction following lower UV doses. Most likely, these fragments were not dephosphorylated at the 3′ end during the treatment with calf intestinal phosphatase. [Staphylococcal nuclease leaves a 3′-phosphate, which is not degraded by T4 polymerase–exonuclease (Hershfield & Nossal, 1972).]

In order to examine changes in this distribution more closely, the 30–130-base section of each autoradiogram was scanned at higher sensitivity (Figure 4B). It is clear that the periodic pattern persists throughout the rapid phase of repair and is present (although attenuated) even after >90% of the PD are removed (see Figure 1). A similar analysis was performed with IMR-90 cells where the fast repair phase is complete by 6 h after irradiation. As shown in Figure 5, a clear periodic pattern is observed following repair times of 0, 6, and 24 h. This latter time corresponds to about 60% removal of PD (data not shown).

In order to quantitatively assess changes in these distributions during repair, the scans were analyzed by a peak deconvolution procedure (Lan & Smerdon, 1985). An example of the results of this analysis for a single scan is shown in Figure 6. As can be seen, the scans are digitized and then fit by a combination of basis spectra which can have both Guassian and Lorentzian character. The deconvoluted spectra (Figure 6C) were then used to determine the relative areas of each ~10-base ensemble in the original scan (i.e., Figure 6A). This was done for the 0-h scans shown in Figures 4 and 5, as well as the 24-h (AG1518 cells) and 6-h (IMR-90 cells) repair times. These latter times correspond to points in the repair time course of each cell type where the fast repair phase is complete (or nearly complete) so the majority of repair occurring at these times is associated with the slow repair phase

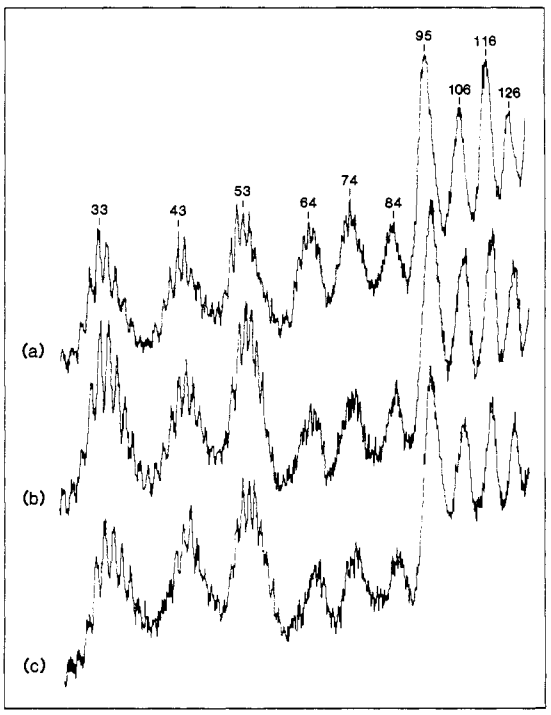

FIGURE 5: Distribution of PD in nucleosome core DNA from IMR-90 cells following different repair times. Scans are for cells that were irradiated and incubated for (a) 0, (b) 6, and (c) 24 h prior to irradiation. See Figure 4 for details.

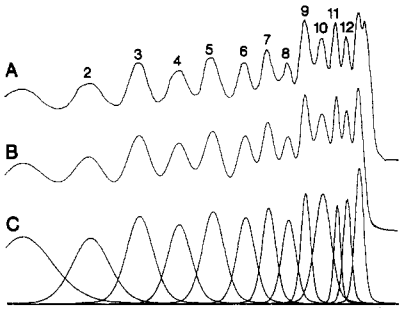

FIGURE 6: Example of curve analysis and peak deconvolution of PD distribution curves for area determinations of the ~10-base ensembles. The digitized profile of a PD map for core DNA from bovine thymus chromatin irradiated at 500 J/m^2 is shown by curve A. Details on the preparation of this sample can be found in Gale and Smerdon (1988). The best fit to curve A using the curve analysis program is shown by curve B. The deconvolution spectra calculated from the best fit is shown in curve C.

(e.g., see Figure 1). A comparison between the two repair times for each cell strain is shown in Figure 7. Although some changes occur in the PD distribution during the fast repair phase (e.g., ensembles 3 and 4 for IMR-90 cells), there is no evidence for selective removal of PD from the end regions of core DNA (discussed earlier) during this phase in either cell type. We conclude that the nonuniform distribution of repair incorporation observed at early times after UV irradiation (Figure 2A) is not the result of a marked selectivity of repair within the core particle.

Comparison of Repair Synthesis and PD Distributions. It is possible that the nonuniform distribution of repair synthesis observed at early times reflects the rather complex distribution of PD in core DNA (e.g., Figures 4 and 5). To assess this possibility, we initially compared the PD distributions of isolated chromatin, irradiated at 500 J/m^2, to the distributions measured for each of the human cell strains (Figure 8). This was done because the chromatin data could be more accurately analyzed (deconvoluted) closer to the 3′ and 5′ ends of the core

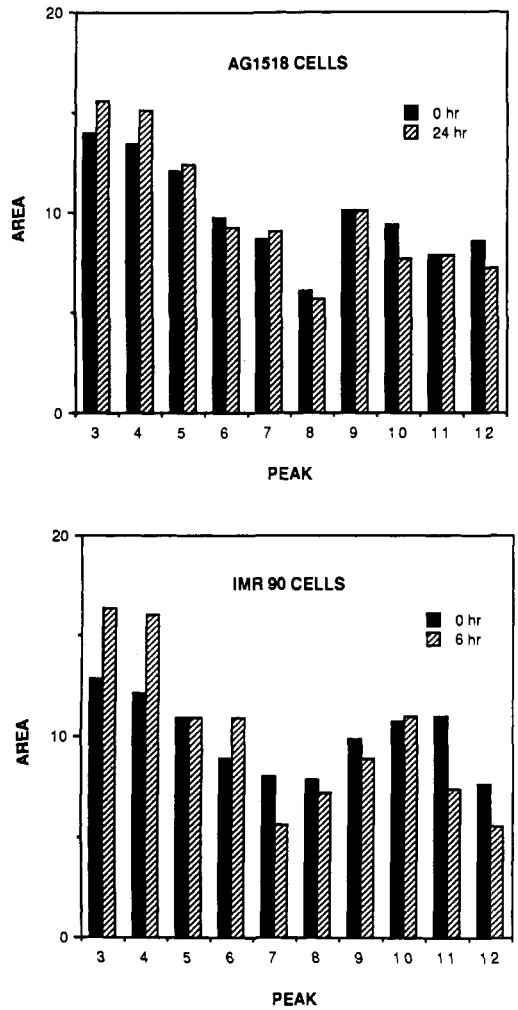

FIGURE 7: Relative yield of PD at ~10-base intervals in nucleosome core DNA from AG1518 cells and IMR-90 cells before and after the fast repair phase. Ordinate values represent the relative areas (in percent) of individual ensemble peaks (i.e., each set of ~10 single base bands forming a peak) in the PD distribution (e.g., Figure 4B) determined as shown in Figure 6. Abscissa values are ensemble peak numbers starting at the 5′ end of core DNA. In each panel, the solid bars give the relative areas of the ensemble peaks immediately after UV irradiation (0 h), and the hatched bars give the relative areas following 24 h (top panel) or 6 h (bottom panel) of repair incubation.

DNA than the scans for the cells, due to the much higher signal obtained at the higher UV dose (Gale & Smerdon, 1988). Therefore, the scans for irradiated chromatin could be used for obtaining values for PD yield at the core DNA ends. As shown in Figure 8, the PD yield at each (~10-base) position, from ensemble 3 to ensemble 12, is relatively similar for the different samples, with the exception of position 11 (114 bases from the 5′ end). [Interestingly, the yield at this position also appeared to vary as the chromatin fiber folds into more compact structures (Gale & Smerdon, 1988).] Therefore, we assumed that the relative PD yield at positions 13 and 14 could be taken from the more accurate chromatin data, and the yield at positions 0, 1, and 2 could be obtained by extrapolation. These assumptions allowed us to calculate the PD distribution throughout the core DNA region (Figure 9A).

Once the entire PD distribution in nucleosomes is known, one can calculate the expected repair patch distribution (see Appendix). To perform this calculation, however, one needs to know the average PD yield of linker DNA and the average repair patch size. We assumed that the yield of PD in linker DNA is equivalent to the *average* PD yield in core DNA (Niggli & Cerutti, 1982; Williams & Friedberg, 1979). The

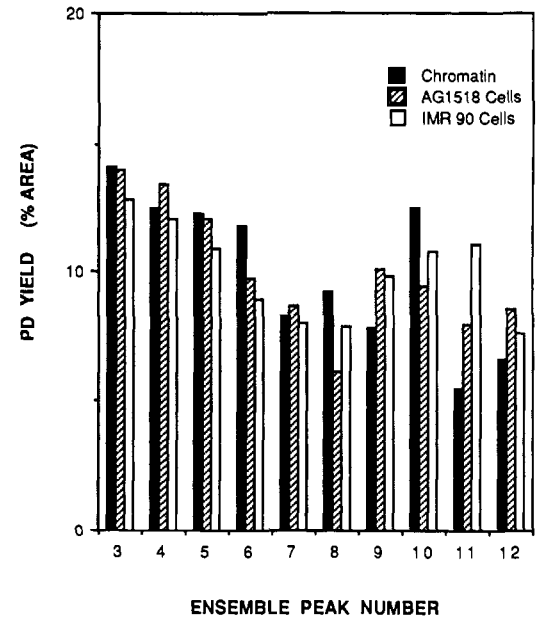

FIGURE 8: Comparison of the relative yields of PD in ~10-base segments in core DNA from UV-irradiated chromatin and UV-irradiated human cells. The data were obtained, as described in Figures 6 and 7, for bovine thymus chromatin irradiated at 500 J/m^2 (Gale & Smerdon, 1988) and each of the human fibroblast strains irradiated at 12 J/m^2 and harvested immediately (no repair).

average patch size for UV-induced repair synthesis has been measured by several laboratories, using the BrdUrd density-shift method, and falls in the range of 20–40 bases (Edenberg & Hanawalt, 1972; Smith, 1978; Th'ng & Walker, 1983; Dresler, 1985; K. Sidik and M. Smerdon, submitted for publication; present report). Therefore, we calculated the distribution of repair synthesis for both of these patch sizes (i.e., $L = 20$ and $L = 40$) that is expected for the PD distribution measured (assuming no selective repair occurs). As shown in Figure 9B, the distribution for either patch size is heavily weighted to the 5′ end, with the lowest predicted incorporation being in the central 73–94-base region. We compared this distribution with the actual exonuclease III mapping data (Figure 2) by transforming the values shown in Figure 9B to values that can be plotted on the same graph as the actual data (Appendix). As can be seen in Figure 10B, the transformed curves from Figure 9B yield good fits to the data except at the very 5′ end. Furthermore, when the higher UV dose PD map (for irradiated chromatin) was used to predict the repair patch distribution, the fits obtained were also quite good for the region from ~40 bases to 146 bases from the 5′ end (Figure 10A). Thus, most of the nonuniform distribution of repair incorporation within core DNA (Figure 2A) can be accounted for by the nonuniform distribution of PD in this region.

Discussion

We reported previously that repair patches inserted during the fast repair phase in human fibroblasts are nonuniformly distributed in nucleosome cores, with a marked bias toward the 5′ end (Lan & Smerdon, 1985). It was shown in that report that a simple distribution, where repair synthesis is devoid in an ~50-base region near the center of core DNA, gives a relatively good fit to the data. As discussed in detail in that report, such selective repair could account for the two repair phases in human cells since these phases may represent rapid repair of the core DNA ends and slow repair of the (less accessible) ~50-base central region. In the present report, we have tested this hypothesis directly by comparing the repair

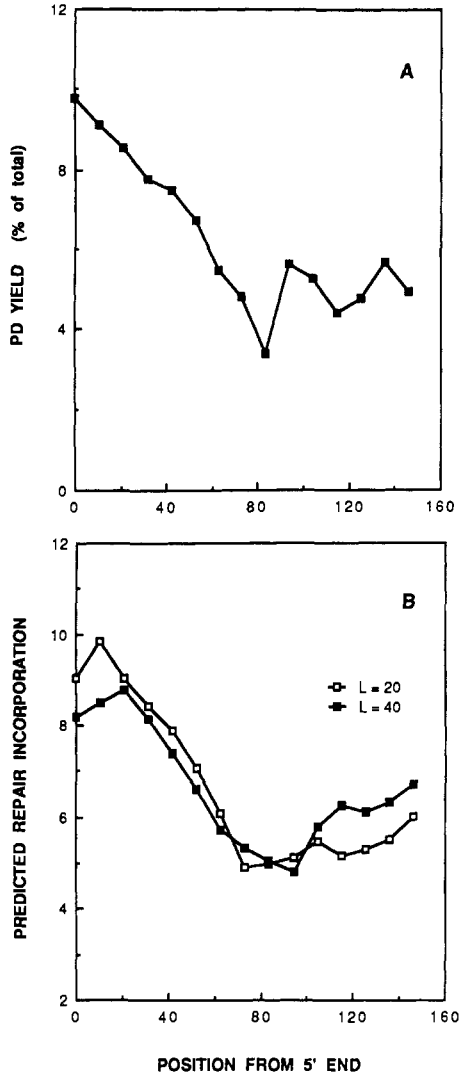

FIGURE 9: Relative yield of PD (A) and predicted repair incorporation (B) at 10.4-base intervals in nucleosome core DNA of AG1518 cells. (A) Values shown for positions 31–125 were determined from peak deconvolution analysis of the PD distribution curve for AG1518 cells harvested immediately after UV irradiation (Figure 4, scan a). The values for positions 136 and 146 were obtained from the deconvolution analysis for UV-irradiated chromatin (see Figure 6), assuming that the relative area of peak 12, and the ratio of heights for these peaks and peak 12 (i.e., $H_{peak\,x}/H_{peak\,12}$), is the same in irradiated chromatin as in irradiated cells. This calculation was necessary, because of the large peak at 146 bases (from undigested DNA) obtained for cells at the lower UV dose (Figure 4A). The values for positions 0, 10, and 21 were obtained from extrapolation of a linear fit to the values measured at positions 31, 42, and 52, and were similar to values obtained for irradiated chromatin. (B) Fraction of repair incorporation in nucleosome core DNA at each position (10.4-base intervals) predicted by the PD distribution shown in panel A, using repair patch sizes of 20 (□) and 40 (■) bases (see eq A2 of Appendix).

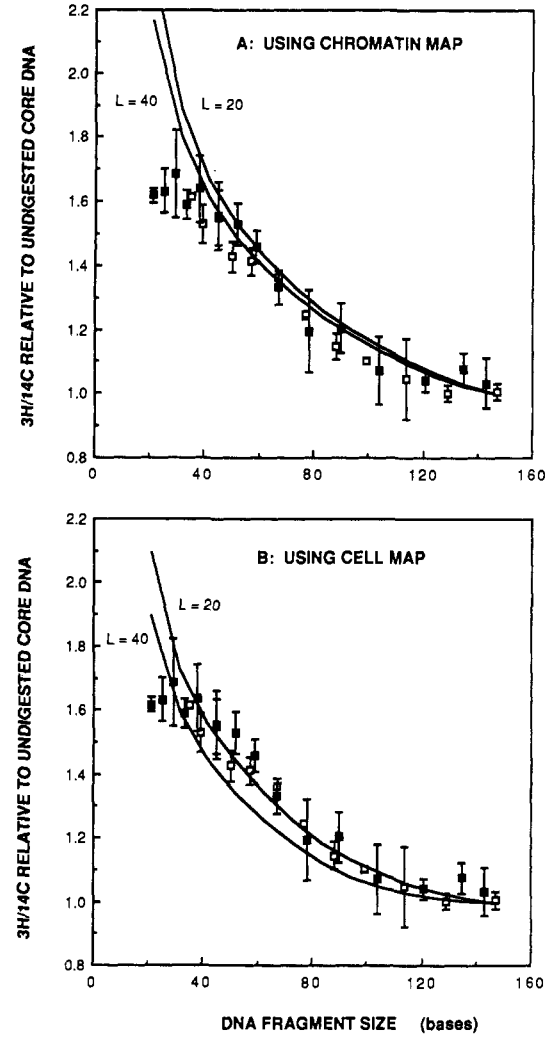

FIGURE 10: Comparison of data measured for the distribution of repair synthesis in nucleosome core DNA with the distributions predicted from the PD distributions obtained for irradiated chromatin (A) and AG1518 cells (B). The data points are from Figure 2A. The symbols are for a 30-min labeling pulse (□) and a 30-min pulse plus 2.5-h chase (■). The predicted curves (solid lines) represent plots of eq A5 (Appendix) for patch sizes of 20 (L = 20) and 40 (L = 40) bases in each panel.

patch and PD distributions in core DNA before and after the fast repair phase. These studies were performed on two different human fibroblast strains. For one of these strains (IMR-90 cells), there is a clear break (at <6 h) between the fast and slow repair phases, while this was not observed for the other strain examined (AG1518 cells). In the latter cells, the fast phase appears to persist for at least 16 h after irradiation and involves removal of ~20% more PD than in IMR-90 cells (Figure 1). Therefore, we were able to test for selective repair in cell strains with (presumably) different combinations of fast and slow repair components.

The results of the repair synthesis mapping studies indicate that the distribution of repair patches in core DNA does indeed change following fast repair (Figure 2). However, the change is to a more uniform distribution, and there is no indication of a bias toward the central region. One possibility for this result is that repair patches could be much longer during the slow repair phase and extend well beyond the PD site being repaired (i.e., they may extend into adjacent nucleosomes). This would result in a population of core DNA molecules with a random (or nearly random) distribution of ^3H (repair) label even though selective repair was occurring. However, the patch size measurements indicate that this is not the case (Figure 3). Indeed, patches inserted during the slow phase are actually shorter (by about half) than those inserted during the fast phase (Table I). This observation does not explain the change in repair patch distribution between the two phases.

Mapping of PD in core DNA following different extents of repair provided a direct test for selective removal of PD within subdomains of the core particle. The results clearly show that no marked selectivity in repair takes place within the 30–130-base region of the core particle during the fast repair phase in either cell strain (Figures 4 and 5). The 10.3-base periodic pattern of PD formation in core DNA persists throughout the fast phase in each cell type, and the relative yield of PD in each ~10-base ensemble gives no

indication of selective removal in the central region during the fast repair phase (Figure 7). However, the nonuniform distribution of repair patches inserted during the fast phase may reflect (at least in part) the nonuniform PD distribution in core DNA. Quantitative analysis of the PD distribution, and the repair patch distribution predicted by this analysis, indicates that this is indeed the case (Figure 9). In fact, a direct comparison of the $^3H/^{14}C$ ratio data, obtained from the exonuclease III mapping studies, and the values expected for the predicted repair patch distribution shows that the measured values are quantitatively similar to those predicted, with the possible exception of the very 5′ end of the core DNA (Figure 10). Thus, the nonuniform distribution of repair synthesis during the fast repair phase in core particle regions can be accounted for by the nonuniform distribution of PD, and there is little evidence for selective repair in this region.

If selective repair does not occur within nucleosome core regions during the fast repair phase, what then is the reason for two repair phases? Furthermore, what is the reason for the different distributions of repair patches in core DNA during fast and slow repair? The following is a list of observations concerning repair of UV damage that should provide clues for answering these questions: (1) Between 50 and 75% of the PD are removed during the fast repair phase in human cells [reviewed in Smerdon (1989)]; (2) the sensitivity of repair patches to exogenous nucleases and the rate of maturation of these patches into nucleosome structures increase during later repair times (Smerdon & Lieberman, 1980); (3) the repair patch distribution in core DNA becomes more uniform and the average patch size decreases during late repair times (present report); and (4) at least some transcriptionally active genes are repaired more rapidly in mammalian cells [reviewed in Bohr et al. (1987)], and this enhanced repair occurs primarily (if not exclusively) in the coding strand (Mellon et al., 1987). Since the fast repair phase involves removal of a majority of PD, it is unlikely that *only* transcriptionally active genes are repaired during the fast phase. However, a much larger fraction of DNA may be associated with "relaxed" chromatin structures or, at most, may require minimal modification to be relaxed (Reeves, 1984). Therefore, an important factor for selective repair in chromatin may be the *degree of compaction* of the nucleofilament. This does not explain, however, observations 2 and 3 above. One possibility is that the enhanced nuclease sensitivity, rapid nucleosome rearrangement, and nearly random distribution of repair patches (following nucleosme rearrangement) reflect either a different alteration or a more "radical" alteration in nucleosome structure during slow repair than occurs during the fast repair phase. For example, nucleosomes in highly compact chromatin may require more extensive unfolding during excision repair and, upon refolding, the core histones attach randomly (relative to their original placement) along the newly repaired DNA. The more rapid refolding could reflect the local environment and/or physical tension of these regions to maintain a highly condensed structure. Alternatively (or in addition), nucleosomes in these regions may require either different or more extensive modifications, such as histone acetylation, to unfold the chromatin fiber for excision repair (Smerdon, 1989). These modifications (or their reversal) may alter the placement of core histones along DNA during the maturation process. In either case "reattachment" of histones to newly repaired DNA at positions different from their original positions would randomize the repair label in core DNA.

The change in repair patch size following fast repair was somewhat surprising, since Smith (1978) had reported that repair patches inserted 12–16 h after UV irradiation in a different human fibroblast strain (WI38) are the same size as patches inserted during the 0–2-h period. One explanation for this apparent contradiction with our results is that the fast repair phase is not complete until later times in WI38 cells, as was observed for AG1518 cells, and 12 h is still within the fast phase. With regard to our results, we initially thought that the change in patch size might reflect the action of different polymerases during the two repair phases. However, Dresler et al. (1988) reported that repair synthesis during early (0–2-h) and late (14–33-h) times after irradiation in AG1518 cells is inhibited by aphidicolin and (butylphenyl)-2′-deoxyguanosine 5′-triphosphate, implicating polymerases α and δ in both repair phases. Therefore, we are led to presume that the change in patch size reflects some other feature of the slow repair phase. Perhaps differences in structural constraints of nucleosomes repaired during the two phases are reflected in the different patch sizes observed.

Finally, it is clear from the data in Figures 4 and 5 that the fast repair phase does not involve selective removal of PD that are on the "outer side" of the core DNA strands (i.e., away from the histone surface). However, it appears that the amplitude of the peaks decreases during the slow phase (Figure 4). Thus, it is possible that selective removal of PD within core DNA occurs during what we have called the slow repair phase. This would suggest that *three* repair phases exist and the slow phase is actually composed of two different rates of repair.

ACKNOWLEDGMENTS

We thank Ahmed Murad for the preparation of T4 endonuclease V used in this study, James Mueller for performing the peak deconvolution analyses, Dr. James Gale for help with the pyrimidine dimer mapping studies, and Jirair Bedoyan for critical reading of the manuscript. Portions of this work were presented at the 1988 UCLA Symposium on Mechanisms and Consequences of DNA Damage Processing.

APPENDIX

This section shows the development of the equations used for predicting the distribution of repair patches in core DNA from the distribution of PD.

Consider the distribution of PD (given in relative areas) at each position (x) from the 5′ end of core DNA, where x represents the center of the ~10-base ensembles (e.g., Figure 8). The number of repair patches at each position (N_x) is

$$N_x = \sum_{i=x-l/2}^{x+l/2} f_i \qquad \text{(A1)}$$

where f_i is the fraction of total PD in core DNA in ensemble i and l is the repair patch size divided by 10.4 bases (e.g., $l = 2$ for a 20-base patch size). For $14 < x < 0$ (i.e., the linker DNA region), the fraction of PD/10.4 bases (f_i) was assumed to be the average value of f_i in the core region (see text). The fraction of total patches overlapping position x is

$$N_x / \sum_{x=0}^{14} N_x \qquad \text{(A2)}$$

To compare the predicted distribution of repair patches with the exonuclease e III data, one must first sum up *all* patches from the 5′ end (0) to each position x along core DNA, or

$$T_{0x} = \sum_{i=0}^{x} N_x \qquad \text{(A3)}$$

where T_{0x} is the total ^3H dpm from position 0 (5′ end) to position x. Normalizing to the fragment length at each position x (L_{0x}) gives

$$(^3H/^{14}C)_x = T_{0x}/L_{0x} = \sum_{i=0}^{x}(N_i/i) \qquad (A4)$$

Finally, to directly compare this distribution to data published in past reports, the values given by eq A4 must be normalized to the $^3H/^{14}C$ value for undigested core DNA [i.e., $(^3H/^{14}C)_{146}$]:

$$\frac{(^3H/^{14}C)_x}{(^3H/^{14}C)_{146}} = \frac{T_{0x}/L_{0x}}{T_{014}/L_{014}} = \frac{\sum_{i=0}^{x}(N_i/i)}{\sum_{i=0}^{14}(N_i/i)} \qquad (A5)$$

References

Bohr, V. A., Phillips, D. H., & Hanawalt, P. C. (1987) *Cancer Res. 47*, 6426–6436.

Chan, G. L., Doetsch, P. W., & Haseltine, W. A. (1985) *Biochemistry 24*, 5723–5728.

Cohn, S. M., & Lieberman, M. W. (1984) *J. Biol. Chem. 259*, 12463–12469.

Doetsch, P. W., Chan, G. L., & Haseltine, W. A. (1985) *Nucleic Acids Res. 13*, 3285–3304.

Dresler, S. L. (1985) *Biochemistry 24*, 6861–6869.

Dresler, S. L., Gowans, B. J., Robinson-Hill, R. M., & Hunting, D. J. (1988) *Biochemistry 27*, 6379–6383.

Edenberg, H., & Hanawalt, P. (1972) *Biochim. Biophys. Acta 272*, 361–372.

Friedberg, E. C. (1985) *DNA Repair*, W. H. Freeman and Co., New York.

Gale, J. M., & Smerdon, M. J. (1988) *J. Mol. Biol. 204*, 949–958.

Gale, J. M., & Smerdon, M. J. (1990) *Photochem. Photobiol. 51*, 411–417.

Gale, J. M., Nissen, K. A., & Smerdon, M. J. (1987) *Proc. Natl. Acad. Sci. U.S.A. 84*, 6644–6648.

Ganesan, A. K., Smith, C. A., & van Zeeland, A. A. (1981) in *DNA Repair, A Laboratory Manual of Research Procedures* (Friedberg, E. C., & Hanawalt, P. C., Eds.) Vol. 1, Part A, pp 89–97, Marcel Dekker, New York.

Hershfield, M. S., & Nossal, N. G. (1972) *J. Biol. Chem. 247*, 3393–3404.

Lan, S. Y., & Smerdon, M. J. (1985) *Biochemistry 24*, 7771–7783.

Linxweiler, W., & Horz, W. (1982) *Nucleic Acids Res. 10*, 4845–4859.

Mellon, I., Spivak, G., & Hanawalt, P. C. (1987) *Cell 51*, 241–249.

Niggli, H. J., & Cerutti, P. A. (1982) *Biochem. Biophys. Res. Commun. 105*, 1215–1223.

Nissen, K. A., Lan, S. Y., & Smerdon, M. J. (1986) *J. Biol. Chem. 261*, 8585–8588.

Paterson, M. C., Smith, B. P., & Smith, P. J. (1981) in *DNA Repair: A Laboratory Manual of Research Procedures* (Friedberg, E. C., & Hanawalt, P. C., Eds.) Vol. 1, Part A, pp 99–111, Marcel Dekker, New York.

Ramanathan, B., & Smerdon, M. J. (1989) *J. Biol. Chem. 264*, 11026–11034.

Reeves, R. (1984) *Biochim. Biophys. Acta 782*, 343–393.

Smerdon, M. J. (1989) DNA Excision Repair at the Nucleosome Level of Chromatin, in *DNA Repair Mechanisms and their Biological Implications in Mammalian Cells* (Lambert, M. W., & Laval, J., Eds.) pp 271–294, Plenum Publishing Corp., New York.

Smerdon, M. J., & Lieberman, M. W. (1980) *Biochemistry 19*, 2992–3000.

Smerdon, M. J., Tlsty, T. D., & Lieberman, M. W. (1978) *Biochemistry 17*, 2377–2386.

Smerdon, M. J., Kastan, M. B., & Lieberman, M. W. (1979) *Biochemistry 18*, 3732–3739.

Smerdon, M. J., Lan, S. Y., Calza, R. E., & Reeves, R. (1982) *J. Biol. Chem. 257*, 13441–13447.

Smith, C. A. (1978) in *DNA Repair Mechanisms* (Hanawalt, P. C., Friedberg, E. C., & Fox, C. F., Eds.) pp 311–314, Academic Press, New York.

Smith, C. A., & Okumoto, D. S. (1984) *Biochemistry 23*, 1383–1391.

Smith, C. A., Cooper, P. K., & Hanawalt, P. C. (1981) in *DNA Repair: A Laboratory Manual of Research Procedures* (Friedberg, E. C., & Hanawalt, P. C., Eds.) Vol. 1, Part B, pp 289–305, Marcel Dekker, New York.

Th'ng, J. P. H., & Walker, I. G. (1983) *Carcinogenesis 4*, 975–978.

Walker, I. G., & Th'ng, J. P. H. (1982) *Mutat. Res. 105*, 277–285.

Williams, J. I., & Friedberg, E. C. (1979) *Biochemistry 18*, 3965–3972.